

Diffusion of He³ in bcc and hcp phases of solid solutions of helium isotopes

V. N. Grigor'ev, B. N. Esel'son, and V. A. Mikheev

Physico-technical Institute of Low Temperatures, Ukrainian Academy of Sciences

(Submitted July 11, 1973)

Zh. Eksp. Teor. Fiz. 66, 321-329 (January 1974)

Results are presented of measurements of the diffusion coefficients D of He³ in bcc and hcp phases of He³-He⁴ solutions with He³ concentrations from 0.25 to 6.3%, using a pulsed NMR technique that has been improved in order to increase the range of the measurements of D . It is shown that in the hcp phase of solid helium, in samples of increased density, the temperature dependence of D is determined by the existence of two diffusion mechanisms (the vacancy mechanism that determines D at high temperatures, and the impuriton quantum diffusion mechanism at low T). In the bcc phase, which is closed for weak solutions, just as in pure He³, the He³ at a concentration x less than 2% diffuses through the vacancies over the entire temperature range. In the bcc phase of a solution with $x=6.3\%$ He³, the diffusion coefficient has a more complicated temperature dependence. A model is proposed to explain this behavior of D . Phase diagrams of weak He³-He⁴ solutions are constructed on the basis of the data on the diffusion coefficient in the bcc-hcp transition.

Investigation of the diffusion of He³ in weak He³-He⁴ solid solutions has recently led to experimental observation of a new phenomenon, namely quantum diffusion^[1,2]. The distinguishing feature of this phenomenon is that at low temperatures the diffusion coefficient of the impurities (D) does not depend on the temperature and varies in inverse proportion to the concentration (x). According to the prevailing theoretical notions, these features are due to the fact that the impurities and defects in quantum crystals behave like quasiparticles, whose motion is determined by their interaction with the phonons and with one another^[3-6].

We present here detailed information on the results of measurements of the diffusion coefficient of He³ in He³-He⁴ solid solutions in the hcp and bcc phases.

MEASUREMENT METHOD AND APPARATUS

The diffusion coefficient was measured by the methods of ordinary and stimulated echo, using a pulsed NMR spectrometer^[7], which was modernized to extend the range of measured values of D . As is well known, in a constant magnetic field H_0 with a gradient G , the phase of the nuclear spin precession varies with the mobility of the nuclei. As shown by Carr and Purcell^[8], when radio-frequency pulses in a sequence $90^\circ - \tau - 180^\circ$ are applied to a spin system in equilibrium, the 180° system-response pulse produced after a time interval τ (the spin-echo signal) is described by the expression

$$h = h_0 \exp \left\{ -2\tau/T_2 - \frac{1}{3}\gamma^2 G^2 D \tau^3 \right\}, \quad (1)$$

where h_0 is the echo signal as $\tau \rightarrow 0$, T_2 is the spin-spin relaxation time, and γ is the gyromagnetic ratio.

An examination of expression (1) with allowance for the real values of the parameters contained therein shows that the use of the ordinary spin-echo method makes it possible to measure reliably $D \geq 10^{-8}$ cm²/sec at $T_2 \geq 100$ msec and $G \approx 20$ G/cm. Measurement of smaller values of D entails a number of difficulties.

New possibilities are afforded in this respect by the use of the three-pulse procedure proposed by Hahn^[9]. When three 90° radio-frequency pulses are applied to a nuclear system in the sequence $90^\circ - \tau_1 - 90^\circ - (\tau_2 - \tau_1) - 90^\circ$, five echo signals are produced at different instants of time. From the point of view of measurements of D , the greatest interest attaches to the so-called "stimu-

lated echo," which is produced at a time τ_1 after application of the third pulse. The stimulated-echo signal amplitude is determined in this case by the expression^[10]

$$h_{st} = \frac{1}{2} h_0 \exp \left\{ -\frac{\tau_2 - \tau_1}{T_1} - \frac{2\tau_1}{T_2} - \gamma^2 G^2 D \tau_1^2 \left(\tau_2 - \frac{\tau_1}{3} \right) \right\}, \quad (2)$$

where T_1 is the spin-lattice relaxation time. If the condition $T_1 > \tau_2 \gg \tau_1$ is satisfied, then the third term of the curly brackets of (2) plays the principal role. Inasmuch as $T_1 \geq 10^3$ sec in solid He³-He⁴ solutions at low temperature^[11], the condition indicated above can easily be satisfied, and the use of the stimulated-echo method can greatly extend the limits of measurable values of D . In the present study, the use of the stimulated-echo method made it possible to measure $D \sim 10^{-10}$ cm²/sec.

The pulsed NMR spectrometer, operating at 9.25 MHz, has been described earlier^[7]. It was improved in the present study by introducing additional blocks, so that operation in the ordinary and stimulated echo modes was made possible. A block diagram of the spectrometer used to obtain the stimulated echo is shown in Fig. 1.

To produce rectangular video pulses we used a standard pulse generator of type G5-15. The time interval τ_1 between the first and second 90° pulses was determined by a master unit (MU). The delay τ_2 of the third 90° pulse was provided by phantastron F-1, which made it possible to vary τ_2 from 1 to 40 sec. The phantastron F-2 was used to delay the triggering of the oscilloscope for the purpose of obtaining a swept echo signal.

The high-frequency amplifier (HFA) used by us had a gain $\sim 5 \times 10^5$ and a bandwidth ~ 150 kHz. The echo sig-

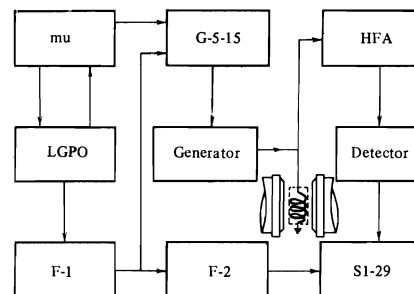


FIG. 1. Block diagram of NMR spectrometer used to obtain stimulated-echo signals.

nal was memorized after amplification and detection by the cathode-ray tube of an S1-29 oscilloscope.

Just as in the case of ordinary echo, when working with stimulated echo the sample was first saturated by a series of pulses so as to equalize the populations of the magnetic sublevels, and the first pair of 90° pulses was applied after a certain time governed by the low-frequency generator of periodic oscillations (LGPO). The block diagram of the spectrometer used to obtain the $90^\circ - \tau - 180^\circ$ sequence did not differ in principle from that described earlier^[7]. In order to verify and compare the operation of the setup in different regimes, the diffusion coefficient was measured at high temperatures using both the ordinary and the stimulated spin-echo methods. Results of measurements by the two methods agreed within limits of the measurement accuracy, namely 5–15%, depending on the value of D .

The magnetic-field gradient was produced with the aid of coils placed in the gap of the permanent magnet, and was determined from the waveform of the echo signal.

The solid-helium samples were obtained by the method of blocking a capillary in a copper cell with a capacitive pressure pickup^[7].

The technique used in our experiments to obtain low-temperatures is well known. To obtain $T < 1.5^\circ\text{K}$ we used a refrigerator with He^3 ^[12], and the temperature was determined from the vapor tension over the liquid He^3 and monitored with a carbon resistance thermometer in thermal contact with the cell of the sample.

RESULTS AND DISCUSSION

1. Phase Diagrams of Weak He^3 - He^4 Solutions

In the investigation of the diffusion coefficient in the bcc and hcp phases of He^3 - He^4 solutions, it is very important to know the phase diagrams of these solutions. At the present time, these data are incomplete for weak solutions of He^3 in He^4 . Measurements of the diffusion coefficients have made it possible to fill this gap in part and to construct phase diagrams of solutions containing 0.75, 2.17, and 6.3% of He^3 (Fig. 2). What is essential here is the fact that the values of the diffusion coefficient in the bcc and hcp phases differ by several dozen times^[13], so that the temperature of the bcc-hcp phase transition can be reliably registered.

As seen from the figure, the regions of the bcc phases at $x = 2.17$ and 0.75% He^3 are closed, just as in the case of pure He^4 . In Fig. 2, the indicated regions are delineated by solid lines. For $x = 6.3\%$ He^3 , the bcc phase exists down to the lowest investigated temperatures, as is also the case for solutions with 5 and 8% He^3 according to data by other authors^[14,15]. It is clearly seen that the bcc-hcp transition temperature is strongly shifted in solutions towards lower temperatures at rather low He^3 concentrations. On the basis of these data we can expect that at $x \approx 4\%$ He^3 the region of existence of the bcc phase will extend all the way to the solid-solution stratification line.

2. Diffusion of He^3 in bcc Phase of He^3 - He^4 Solutions

The diffusion of He^3 in solutions containing 0.75, 2.17, and 6.3% He^3 was investigated in the entire temperature region of the existence of the bcc phase. At temperatures 2.0–1.0°K, the diffusion coefficient of these solu-

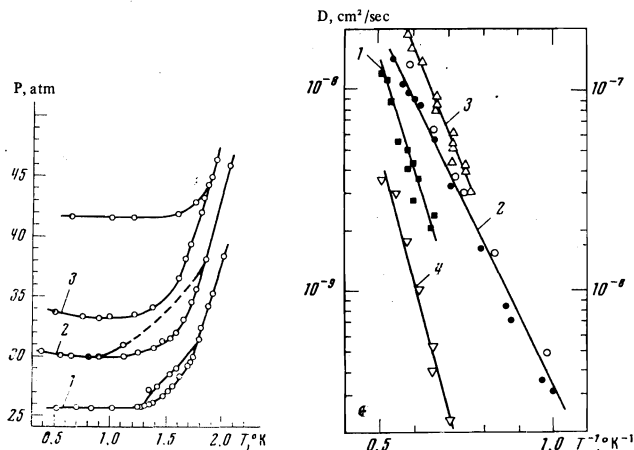


FIG. 2

FIG. 2. Phase diagrams of He^3 - He^4 solutions: 1—0.75%, 2—2.17%, 2—6.3% He^3 . Diagrams 2 and 3 are shifted relative to 1 by 4 and 8 atm, respectively.

FIG. 3. Dependence of the diffusion coefficient of He^3 on the reciprocal temperature (the ordinate on the right-hand side pertains to the bcc phase, lines 1, 2, 3; the left ordinate pertains to the hcp phase, line 4). ■— He^3 , data of [15], $V = 21.1 \text{ cm}^3/\text{mole}$; ●—6.3%, ○—2.17% He^3 , $V = 21.0 \text{ cm}^3/\text{mole}$; △—0.75% He^3 (data along the melting line); ▽—2.17% He^3 , hcp phase, $V = 20.5 \text{ cm}^3/\text{mole}$.

x, He^3	$V, \text{cm}^3/\text{mole}$	$\Delta, ^\circ\text{K}$	$D_0 \times 10^4, \text{cm}^2/\text{sec}^*$	Note
bcc				
100	21.1	11.7 ± 1.2	4.3 ± 3.4	From data of [15] Results of measurements along the melting line
6.3	21.0 ± 0.05	8.3 ± 1	1.2 ± 1	
2.17	21.0 ± 0.05	8.3 ± 1	1.2 ± 1	
0.75	—	10.5 ± 1	9 ± 4	
hcp				
2.17	20.7 ± 0.05	9.8 ± 1	0.07 ± 0.05	
2.17	20.5 ± 0.05	14.0 ± 1	0.2 ± 0.15	
0.75	20.7 ± 0.05	8.9 ± 1	0.06 ± 0.05	

*Owing to the experimental $D(T)$ dependence, the errors “+” and “-” of the parameter D_0 are not equal. The table lists the larger values.

tions has an exponential decrease with decreasing temperature, in accordance with $D = D_0 e^{-\Delta/t}$, thus confirming the vacancy mechanism of the diffusion.

The measurement results are shown in Fig. 3 and in the table. The straight line 1 in Fig. 3 corresponds to the data of Reich^[16] for pure He^3 . The line 2 illustrates the results for the solutions with 2.17 and 6.3% He^3 , the difference between which lies within the limits of experimental error.

For the solution with 0.75% He^3 (line 3), the interval of the existence of the bcc phase at constant V is very narrow ($\lesssim 0.2^\circ\text{K}$), making it difficult to determine the parameters Δ and D_0 . We therefore performed measurements along the melting curve in the entire region of the existence of the bcc phase (1.3 – 1.8°K)^[1]. Under these conditions, the molar volume increases somewhat with decreasing temperature (from 20.9 to $21.1 \text{ cm}^3/\text{mole}$), leading to an underestimated value of Δ , which nevertheless is larger than in solutions with 2.17 and 6.3% He^3 .

As follows from Fig. 3 and from the table, the behavior of the diffusion coefficient of He^3 in He^3 - He^4 solutions has a number of singularities in comparison with pure He^3 . Attention is called first to the fact that Δ is

much smaller in the solutions than in He^3 , at practically the same value of V . Since identical molar volumes of the He^3 samples and of the solutions correspond to different pressures, the decrease of Δ in the solutions may be due to the decrease in the contribution made to the vacancy-formation energy by the terms that take into account the work of the expansion of the crystal when vacancies are produced in it. In addition, the exponential decrease of D in the He^3 - He^4 solutions continues to very low temperatures and to very low values. It is natural to attribute the latter to the appreciable decrease in the role of the He^3 - He^3 exchange in solid solutions, which leads in pure He^3 to a temperature-independent D at $D \sim 10^{-8} \text{ cm}^2/\text{sec}$.

The existence of a bcc region at $x = 6.3\%$ He^3 down to the lowest investigated temperatures has made it possible to obtain the complete temperature dependence of the diffusion coefficient of He^3 ($V = 21.15 \text{ cm}^3/\text{mole}$). We can distinguish here (Fig. 4) three characteristic sections: 1—exponential $D(T)$ dependence corresponding to the vacancy mechanism, 2—transition section at $0.65 \leq T \leq 1.0^\circ\text{K}$, 3— $D = \text{const}$ at $T < 0.65^\circ\text{K}$.

An analysis of the results suggests, as a working hypothesis, the following possible explanation of this behavior of the diffusion coefficient. In addition to the vacancy mechanism (D_V), which is decisive at high temperatures, two other mechanisms are possible at low temperatures and are connected with the tunneling effect: He^3 - He^4 (D_{34}) and He^3 - He^3 (D_{33}). For weak solutions, owing to the small probability that the He^3 atoms are nearest neighbors, the contribution made to the diffusion by the He^3 - He^3 exchange can become significant only in conjunction with other mechanisms, such as He^3 - He^4 and He^3 -vacancy exchange. Figure 5 shows a scheme in which these mechanisms are combined and which describes the different possibilities for the diffusion displacement of the He^3 atoms. Assuming, in accordance with the hypothesis that the different mechanisms are independent, that the diffusion coefficients are additive for the processes that take place in parallel, and that their reciprocals are additive for processes in succes-

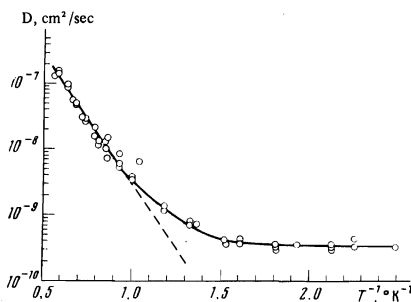


FIG. 4. Temperature dependence of D for $x = 6.3\%$ He^3 , $V = 21.15 \text{ cm}^3/\text{mole}$. The dashed line is an extrapolation of the vacancy section.

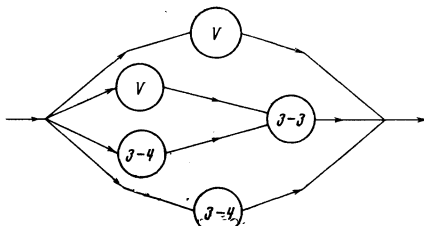


FIG. 5. Scheme of possible diffusion processes. V) diffusion of He^3 via vacancies, 3-4) He^3 - He^4 exchange, 3-3) He^3 - He^3 exchange.

sion, we obtain the following expression for the effective diffusion coefficient:

$$D = (D_v + D_{31}) \left(1 + \frac{D_{33}x}{D_v + D_{34} + D_{33}x} \right). \quad (3)$$

We note that formula (3) can also be easily obtained if one uses the formal analogy of the scheme of Fig. 5 to an electric circuit consisting of resistors, regarding D as the analog of the conductivity. The obtained formula yields the correct expressions for the diffusion coefficient in the limits of high and low temperatures, namely $D \approx D_V$ at high temperatures, inasmuch as $D_V \gg D_{34} \sim D_{33}x$, in this case, while at low temperatures we have $D_V \rightarrow 0$ and

$$D = D_{31} [1 + D_{33}x / (D_{34} + D_{33}x)]. \quad (4)$$

Expression (4) makes it possible to determine D_{34} from the experimental data. Using the expression given for D_{33} of pure He^3 by others^[11, 18]

$$D_{33} = 4.4 (I_{33}/2\pi) a^2,$$

(a is the distance between the nearest neighbors and I_{33} is the He^3 - He^3 exchange integral; in $\text{He}^3 = \text{He}^4$ solutions I_{33} does not depend on the He^3 concentration according to the data of Miyoshi et al.^[15]), and the experimental value of D for $T < 0.65^\circ\text{K}$, we obtain in accordance with (4) $D_{34} \approx 2 \times 10^{-10} \text{ cm}^2/\text{sec}$. Calculation of the diffusion coefficient by formula (3) for the entire investigated temperature range yields satisfactory agreement with the obtained experimental data.

3. Quantum Diffusion of Impuritons in the hcp Phase at Increased Density

Owing to the use of the stimulated-echo procedure, we were able to measure in this study the diffusion coefficient of He^3 in solid-helium samples at increased density. The measurements were carried out in the hcp phase of solutions containing 0.25, 0.75, and 2.17% He^3 , at a molar volume $20.7 \text{ cm}^3/\text{mole}$. We note that the use of this procedure has made it possible to refine the previously obtained data for $V = 21.0 \text{ cm}^3/\text{mole}$.

The dependence of D on the reciprocal temperature for $V = 20.7 \text{ cm}^3/\text{mole}$ is shown in Fig. 6. In contrast to the results obtained in experiments near the melting point, in this case two temperature regions become clearly pronounced as the He^3 concentration is increased, namely, a high-temperature region corresponding to vacancy diffusion, and a low-temperature region where the diffusion coefficient does not depend on the temperature and is determined by the scattering of the impurity quasiparticles by one another. The parameters Δ and D_0 for the vacancy sections of the solutions with 0.75 and 2.17% He^3 are listed in the table.

With decreasing He^3 concentration, owing to the increase of D at low temperatures, the region of vacancy diffusion becomes narrower, as can be seen for $x = 0.25\%$ He^3 , making the determined values of Δ and D_0 unreliable. The values of Δ and D_0 in the hcp phase cannot be compared directly with the analogous parameters for pure He^3 , which has no hcp phase with this value of the molar volume. One can only indicate that Δ in the hcp phase of He^3 - He^4 solutions, just as in the bcc phase, is much smaller than the values of Δ in pure He^3 extrapolated to the given value of V . A comparison of the experimental data for the solution with 2.17% He^3 that correspond to the molar volumes $20.5 \text{ cm}^3/\text{mole}$ (line 4 of Fig. 3) and $20.7 \text{ cm}^3/\text{mole}$ point to a strong dependence of the activation energy in the hcp phase on the density.

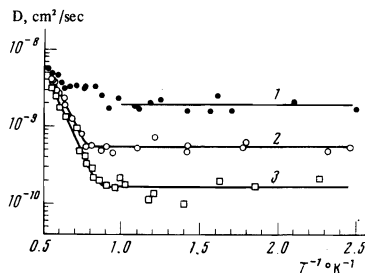


FIG. 6. Dependence of the diffusion coefficient of He^3 on T^{-1} in the hcp phase at $V = 20.7 \text{ cm}^3/\text{mole}$; 1-0.25%, 2-0.75%, 3-2.17% He^3 .

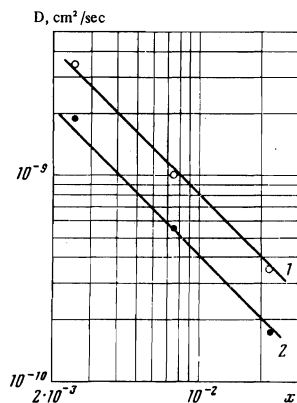


FIG. 7. Concentration dependence of D in the hcp phase at low temperatures: 1) $V = 21.0 \text{ cm}^3/\text{mole}$, 2) $V = 20.7 \text{ cm}^3/\text{mole}$. The line 1 is described by the equation $D = 8.1 \times 10^{-12} x^{-1} \text{ cm}^2/\text{sec}$.

The values of D at low temperatures increase with decreasing concentration like x^{-1} , thus confirming the applicability of the quasiparticle description of the behavior of the He^3 impurities in solid He^4 (Fig. 7)²⁾. Figure 7 shows the concentration dependences of D for $V_1 = 21.0 \text{ cm}^3/\text{mole}$ (line 1) and $V_2 = 20.7 \text{ cm}^3/\text{mole}$ (line 2), where the values of D are obtained by averaging all the points for a given V and x at $T < 1.0^\circ\text{K}$.

Using the relation^[5-7]

$$D \sim I_{34} a^2 / \hbar x, \quad (5)$$

we can estimate the change of I_{34} with changing molar volume. Assuming that the proportionality coefficient in (5) remains unchanged, we have

$$D(V_1)/D(V_2) \approx I_{34}(V_1)/I_{34}(V_2) \approx 1.9, \quad (6)$$

thus indicating a much stronger dependence of I_{34} on the density than for the exchange integral I_{33} (in pure He^3 such a change of V corresponds to a 25% change in the integral I_{33}).

Thus, we have demonstrated that in the bcc phase of weak $\text{He}^3 - \text{He}^4$ solid solutions with $x \leq 2\%$ He^3 the vacancy mechanism of He^3 diffusion is predominant in the entire region in which this phase exists. At $x = 6.3\%$, the temperature dependence of D can be explained by assuming a superposition of three different mechanisms—vacancy diffusion and diffusion via $\text{He}^3 - \text{He}^4$ and $\text{He}^3 - \text{He}^3$ tunneling.

Investigations of increased-density samples in the hcp phase have shown that at high temperatures the

vacancy mechanism is the principal one, and at low temperatures there is quantum diffusion of the impurities. The experimental data have yielded information on the dependence of I_{34} on the density of solid-helium samples.

In conclusion, the authors thank V. A. Slyusarev and M. A. Strzhemechnyĭ for useful discussions and Yu. E. Shul'man for help with the measurements.

¹⁾ Reich [16] has shown that in pure He^3 D does not depend on the temperature on the melting curve, thus confirming the concluded existence of the law of corresponding states [17] in the form $\ln D \sim T_m/T$. This law holds in the case of a linear dependence of the melting pressure (P_m) on the temperature (T_m). As shown earlier, [13] this law does not hold in weak solutions of helium isotopes below 2.0°K .

²⁾ It should be noted that the obtained concentration dependence can also be described, with somewhat poorer accuracy, by the relation $D \sim x^{-4/3}$ obtained by Landesman and Winter [19].

¹⁾ V. N. Grigor'ev, B. N. Esel'son, V. A. Mikheev, and Yu. E. Shul'man, *ZhETF Pis. Red.* **17**, 25 (1973) [*JETP Lett.* **17**, 16 (1973)].

²⁾ M. G. Richards, J. Pope and A. Widom, *Phys. Rev. Lett.* **29**, 708, 1972.

³⁾ A. F. Andreev and I. M. Lifshitz, *Zh. Eksp. Teor. Fiz.* **56**, 2057 (1969) [*Sov. Phys.-JETP* **29**, 1107 (1969)].

⁴⁾ R. A. Guyer and L. I. Zane, *Phys. Rev. Lett.* **24**, 660, 1970.

⁵⁾ V. A. Slyusarev and M. A. Strzhemechnyĭ, *Fizika nizkikh temperatur (Physics of Low Temperatures)*, *Trudy FTINT AN UkrSSR*, No. 19, 67 (1972).

⁶⁾ A. Widom and M. G. Richards, *Phys. Rev. A* **6**, 1196, 1972.

⁷⁾ V. N. Grigor'ev, B. N. Esel'son, V. A. Mikheev, V. A. Slyusarev, M. A. Strzhemechnyĭ, and Y. E. Shulman, *J. Low Temp. Phys.* **13**, No. 1/2, 65, 1973.

⁸⁾ H. Y. Carr and E. M. Purcell, *Phys. Rev.* **94**, 630, 1954.

⁹⁾ E. L. Hahn, *Phys. Rev.* **80**, 580, 1950.

¹⁰⁾ D. E. Woessner, *J. Chem. Phys.* **34**, 2057, 1961.

¹¹⁾ R. A. Guyer, R. C. Richardson and L. I. Zane, *Rev. Mod. Phys.* **43**, 532, 1971.

¹²⁾ B. N. Esel'son, B. G. Lazarev, and A. D. Shvets, *Prib. Tekh. Eksp.*, No. 3, 198 (1962).

¹³⁾ V. N. Grigor'ev, B. N. Esel'son, and V. A. Mikheev, *Zh. Eksp. Teor. Fiz.* **64**, 608 (1973) [*Sov. Phys.-JETP* **37**, 309 (1973)].

¹⁴⁾ J. G. Vignos and H. A. Faribank, *Phys. Rev.* **147**, 185, 1966.

¹⁵⁾ D. S. Miyoshi, R. M. Cotts, A. S. Greenberg, and R. C. Richardson, *Phys. Rev.* **A2**, 870, 1970.

¹⁶⁾ H. A. Reich, *Phys. Rev.* **129**, 630, 1963.

¹⁷⁾ S. A. Rice and N. H. Nachtrieb, *J. Chem. Phys.* **31**, 139, 1959.

¹⁸⁾ J. R. Thompson, E. R. Hunt, and H. Meyer, *Phys. Lett.* **25A**, 313, 1967.

¹⁹⁾ A. Landesman and J. M. Winter, *Calculation of the Diffusion Rate of He^3 Impurities in Solid He^4* , Preprint, Saclay, 1972.

Translated by J. G. Adashko

33